Comparison of new photorefractive composites based on a poly(phenylene vinylene) derivative with traditional poly(*n*-vinylcarbazole) composites

E. Mecher,[a] C. Bräuchle,[a] H. H. Hörhold,[b] J. C. Hummelen[c] and K. Meerholz*[a]

[a] *Physical Chemistry Department, University of Munich, Sophienstr. 11, D-80333 Munich, Germany*
[b] *Institute of Organic and Macromolecular Chemistry, University of Jena, Humboldtstr. 10, D-07743 Jena, Germany*
[c] *Stratingh Institute and Materials Science Centre, University of Groningen, Nijenborgh 4, NL 9747 AG Groningen, The Netherlands*

Received 14th December 1998, Accepted 4th February 1999

The performances of two classes of photorefractive polymer composites with low glass-transition temperatures (about 10–5 °C) are compared. One is based on the commonly used photoconductor poly(*N*-vinylcarbazole) (PVK), *i.e.*, containing isolated charge-transport moieties for hopping. The other is based on the π-conjugated poly[1,4-phenylene-1,2-di(4-benzyloxyphenyl)vinylene] (DBOP-PPV), promising faster response times. The steady-state performance of the DBOP-PPV-based composites was found to be superior owing to (i) the larger internal free volume, allowing more efficient poling of the chromophores, and (ii) the slightly stronger space-charge field as a result of an increased trap density. By contrast, the dynamic response in a four-wave mixing experiment was similar to that of PVK-based composites despite the higher hole-drift mobility in conjugated PPV homopolymers than PVK. It was demonstrated that this is mainly a result of the poor charge-carrier generation efficiency.

1 Introduction

The photorefractive (PR) effect refers to a spatial modulation of the refractive index of refraction generated by a specific mechanism: charge carriers, photogenerated by a spatially modulated light intensity pattern, separate by drift and diffusion processes and become trapped to produce a non-uniform space-charge distribution. The resulting internal space-charge field then modulates the refractive index *via* electrooptic (EO) effects to create a diffractive grating (hologram). Owing to the non-local nature of the grating (*i.e.*, the maxima of the light intensity pattern and the index modulation are out of phase), these materials exhibit energy transfer between the writing beams (so-called "two-beam coupling", TBC). The PR effect is considered today to be one of the most promising mechanisms for many potential holographic applications, including high-density storage, real-time image processing and phase conjugation, because the writing process is reversible and requires only low light intensities.

Among the PR materials in general (*i.e.*, inorganic crystals such as lithium niobate or barium titanate, semiconductors, and organics in general), organic amorphous PR glasses are considered to be particularly promising, because devices can be produced with high reproducibility and at low cost.[1–6] Owing to the necessity to apply electric fields (see below), the organic PR devices are relatively thin (50–200 μm), preventing the use of multiplexing recording schemes for high-density holographic storage. Therefore, the potential use of these materials is directed more towards the real-time domain, *e.g.*, for interferometry or pattern recognition applications.

While the steady-state performance of many PR polymers far exceeds the requirements for real-time holography (Δ*n* values approaching 10^{-2} have been reported for a number of materials,[7–11] allowing complete internal diffraction even in thin devices), the holographic build-up times delimiting the optical data processing speed currently remain too slow to be competitive with computational methods. The fastest time reported is about 5 ms.[12] Current efforts worldwide are devoted to understanding the details of the grating build-up process in amorphous organic PR materials and to improving their holographic response.

The currently best organic PR materials possess glass-transition temperatures (T_g) close to room temperature.[1–12] This permits the *in situ* poling of the dipolar "chromophores", which are responsible for the translation of the electric field into a refractive index modulation Δ*n*, and gives rise to the so-called "orientational enhancement mechanism" (OEM[13]). The formation of the PR refractive index grating in such materials can therefore be formally divided into two steps: (i) the generation of the spatially non-uniform space-charge field (which again consists of two processes, the photogeneration of charge carriers and their redistribution) and (ii) the rotational motion of the chromophores towards the modulated orientation in OEM. Depending on the material's internal free volume (for which T_g might be regarded as a good measure),[14,15] the temperature[16] and the recording conditions (electric field strength, light intensity, geometry, *etc.*), either one of the two processes can be limiting for the holographic response time. In soft "low-T_g" materials, where the orientation is relatively fast, the grating build-up is limited by the space-charge grating formation.[15] This is the case for many of the "fast" PR materials known to date. Therefore, research has to be focused on finding more suitable photoconductor/sensitizer combinations than those currently used. So far, all "fast" (<1 s) organic PR materials contain isolated charge-transport moieties for hopping, typically referred to as "sites".[17] In

most cases, these sites are carbazole units such as in the most commonly used photoconducting polymer poly(*N*-vinylcarbazole) (PVK)[7,9–16] and other carbazole containing polymers.[18] Other candidates that have been utilized for photoconduction in the organic PR field include 4-diethylaminobenzaldedyde diphenylhydrazone (DEH)[19] and triarylamines.[20] These structural motives have also been used in "bifunctional" chromophores, providing EO response and charge transport in one molecule.[21] Little work in the organic PR field has been devoted to π-conjugated polymers, which are known to be better photoconductors owing to the possibility of delocalizing charges along one polymer chain without hopping. Only Yu *et al.*[22] have reported a fully functionalized π-conjugated polymer showing photorefractivity without an applied electric field. This approach was chosen to prevent phase separation, which may occur with the PR composites, but it also has the disadvantages that a single compound has to exhibit all the properties required for the PR effect equally well, which is unlikely, and that optimization of such materials is difficult and time consuming owing to a complicated chemical synthesis. Therefore, PR composites still seem preferable to fully functionalized PR polymers.

Here, we used for the first time a π-conjugated polymer, the PPV derivative poly[1,4-phenylene-1,2-di(4-benzyloxyphenyl) vinylene] (DBOP-PPV;[23] see Fig. 1), as the photoconducting host matrix in a PR composite. DBOP-PPV is an amorphous, high molecular mass polymer (see Table 1 for details). It was prepared by reductive coupling (dehalogenation polymerization) of an appropriately substituted tetrachloride as described previously[23] for a series of analogous phenyl-substituted PPV derivatives. By choosing this ether-derivatized PPV we not only hoped for a faster holographic response as a result of the improved photoconductivity,[24] but we also expected better compatibility with the eutectic (1 : 1) chromophore mixture of 2,5-dimethyl-(4-*p*-nitrophenylazo) anisole (DMNPAA) and 3-methoxy-(4-*p*-nitrophenylazo) anisole (MNPAA)[25] owing to the similar structural motives (diphenylazo ≈ PPV) and the presence of the anisole methoxy group.

In order to take real advantage of the promising photoconducting properties of DBOP-PPV, T_g should be as low as possible (but with sufficient dielectric strength) such that the orientation of the chromophores is faster than the build-up of the space-charge field. Therefore, in addition to the photoconducting polymer and the chromophore mixture, the material contained a plasticizer to adjust T_g and a photosensitizer for charge generation. The goal of this study was then to compare the dynamic and quasi-steady-state PR performance of the DBOP composites with PVK-based composites with similar T_g and the same chromophores and content.

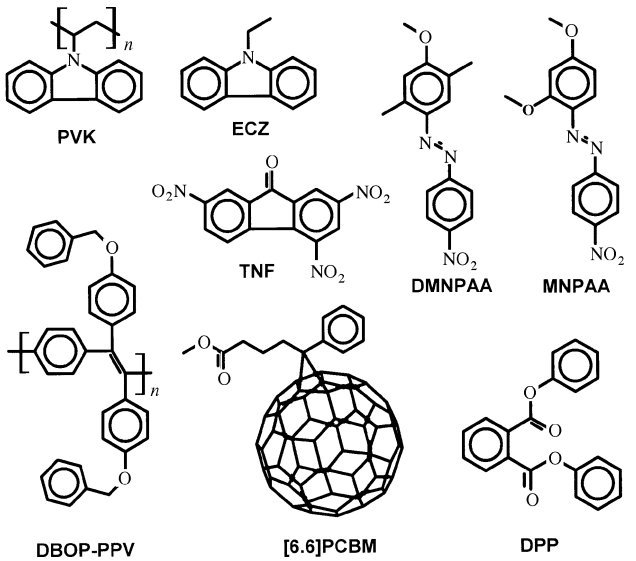

Fig. 1 Structures of the components used in the two PR composites studied: poly[1,4-phenylene-1,2-di(4-benzyloxyphenyl)vinylene] (DBOP-PPV), poly(*N*-vinylcarbazole) (PVK), 2,5-dimethyl-(4-*p*-nitrophenylazo)anisole (DMNPAA), 3-methoxy-(4-*p*-nitrophenylazo) anisole (MNPAA), *N*-ethylcarbazole (ECZ), diphenyl phthalate (DPP), 2,4,7-trinitro-9-fluorenone (TNF) and [6,6]-phenyl-C_{61}-butyric acid methyl ester ([6,6]PCBM).

Table 1 Physical properties of the photoconducting host polymers

Parameter[a]	DBOP-PPV	PVK
λ_{max}/nm	370[23]	340
$M_n(M_w)$/g mol^{-1}	16 300 (40 500)[23]	? (1 100 000)
T_g/°C	143[23]	200
E_{ox}/V *vs.* Ag/AgCl	1.01[23]	1.10
α/cm^{-1}	6	0

[a] Wavelength of maximum absorption λ_{max}, number- and mass-average molecular mass $M_n(M_w)$ as determined by gel permeation chromatography, glass-transition temperatures T_g, oxidation potential E_{ox} determined by cyclic voltammetry and absorption at 633 nm.

The two material classes compared here are not only based on different photoconducting polymers, but also contain different plasticizers [diphenyl phthalate (DPP) for DBOP-PPV and *N*-ethylcarbazole (ECZ) for PVK respectively]. The rationale for using ECZ (= repetitive unit of PVK) as a plasticizer for PVK is (1) its excellent compatibility, (2) its identical polarity and (3) not to reduce the photoconductive properties of the matrix.[3,7] An analogous plasticizer was not available for DBOP-PPV. We used DPP, because it has good compatibility with DBOP-PPV. PR characteristics are complex phenomena which are influenced by the properties of each component and interactions between the components. Since we used different kinds and amounts of plasticizers for the two polymers in this study, we do not discuss the influence on the PR performances of two different photoconducting polymers in a fixed ensemble of chromophores, plasticizer and sensitizer, but the final composites. Two kinds of sensitizers were used, the soluble fullerene derivative [6,6]-phenyl-C_{61}-butyric acid methyl ester ([6,6]PCBM)[26] and 2,4,7-trinitro-9-fluorenone (TNF). All chemical structures are shown in Fig. 1.

Seven materials were investigated, allowing us to compare DBOP-PPV/PCBM-based composites with the PVK/TNF-based analogues of either identical T_g (named II and IV, see Table 2), identical orientational dynamics (II/V), identical sensitizer absorption (II/V), and identical number density of sensitizer (III/V). Additionally, two materials without sensitizer were prepared (I and VII). Finally, PVK was also sensitized with PCBM (VI) to allow comparison of the charge generation process in the two matrices. We did not attempt to sensitize DBOP-PPV with TNF since they do not form a

Table 2 Compositions of the investigated materials (% mm)

	I	II	III	IV	V	VI	VII
Chromophores—							
DMNPAA	20	20	20	20	20	20	20
MNPAA	20	20	20	20	20	20	20
Polymers—							
DBOP-PPV	54.5	54	52				
PVK				51	49	49	50
Plasticizers—							
DPP	5.5	5	5				
ECZ				8	10	10	10
Sensitizers—							
PCBM		1	3			1	
TNF				1	1		

charge-transfer complex like carbazole/TNF, *i.e.*, do not show additional absorption at the desired wavelength.

As an experimental tool to study the materials we performed degenerate four-wave mixing (DFWM) experiments, because they simulate the most promising applications for PR polymers such as optical correlation and time-average interferometry. Furthermore, the comparison of different materials is simple because the diffraction efficiency is determined solely by the index modulation amplitude Δn of the recorded hologram [for constant experimental conditions, see below, eqn. (2)]. Other researchers have been using the so-called "two-beam coupling" (TBC) technique to determine the response time of their materials. However, the interpretation of the TBC data is not straightforward because Δn and also the phase shift ϕ between the light intensity pattern and the recorded index modulation play a role, and their trends may not be the same. Therefore, TBC is a special property of PR materials which can be exploited for phase conjugate applications, for example, but it is not well suited to compare the general performance of PR materials unless the phase shift is also determined in a time resolved fashion.

2 Experimental

The exact compositions of the investigated materials are given in Table 2. For mixing, all components (Fig. 1) were dissolved in methylene chloride, and the solvent was then allowed to evaporate. The glass-transition temperatures were determined by differential scanning calorimetry (DSC) (Mettler Toledo, Model 821e) by first heating the materials to 180 °C and then cooling them to −50 °C. This equilibrates the materials thermal history. After this, the regular temperature ramp was applied at 20 K min^{-1}. For device preparation, the composite was melt-pressed between two ITO-coated glass substrates at elevated temperature using glass spacer beads to adjust the film thickness d. The absorption coefficients at the laser wavelength (633 nm; see below) were measured in 37 μm thick devices using a Kontron Uvikon 860 spectrometer. We report the total absorption coefficient α_t as determined using a non-absorbing dummy cell. Also, we determined the absorption of the sensitizer α_s by using a sample without sensitizer as reference. To obtain the real sensitizing absorption of the DBOP-PPV-based composites, the absorption of the polymer itself had to be added to the α_s values. The polymer absorption was determined by subtracting the absorption of the chromophore mixture (5 cm^{-1}) from the absorption of the DBOP-PPV-based material (I). It was assumed that this number (3 cm^{-1}) is constant for all DBOP-PPV-based materials.

Holographic experiments were carried out at 21 °C (temperature set on our air conditioning system) in the typical tilted geometry[1–6] by overlapping two s-polarized writing beams ('1' and '2', respectively, $\lambda = 633$ nm) in 105 μm thick devices. The external angles (intensities) were $\alpha_{1,\,ext} = 50°$ ($I_{1,\,ext} = 127$ mW cm^{-2}) and $\alpha_{2,\,ext} = 70°$ ($I_{2,\,ext} = 178$ mW cm^{-2}). The recorded grating was read by a weak ($I_{R,\,ext} = 3$ mW cm^{-2}) independent reading beam ($\lambda =$ 633 nm, p-polarized) counter-propagating to write beam '1'. The transmitted and diffracted beams were measured by independent photodetectors. The internal diffraction efficiency η_{int} was calculated according to:

$$\eta_{int} = I_{R,\,diffr}/(I_{R,\,diffr} + I_{R,\,transm}) \quad (1)$$

This definition eliminates the field-dependent absorption and reflection losses and, thus, allows a more straightforward evaluation of the data. According to the coupled-wave theory,[27] η_{int} can be approximated by

$$\eta_{int} \approx \sin^2(C_{FWM}\,\Delta n) \quad (2)$$

with $C_{FWM} = \pi d/[\lambda_0 \cos(\alpha_{1,\,int})]$.

In order to study the poling process independently from the PR grating formation, we determined the changes of the bulk refractive index owing to the induced birefringence and the electrooptic effect by an ellipsometric (ELP) technique.[15,28] For this purpose, a laser beam (780 nm, 80 mW cm^{-2}) was incident under an external angle $\Theta_{ext} = 60°$ with respect to the sample normal. Its polarization was set to +45° and the transmitted light was probed through a −45° polarizer. In order to compensate for the birefringence induced by the non-poled samples, a Soleil–Babinet compensator was placed between the sample and the second polarizer. When no field was applied the PR material did not affect the polarization state of the probe beam (random orientation of the chromophores), and the second polarizer blocked all the transmitted light. With the electric field applied, the transmission T through the second polarizer is given by

$$T_{ELP} = \sin^2(C_{ELP}\,\Delta n') \quad (3)$$

where $\Delta n = n_p - 24n_s$ is the difference between the bulk refractive indices for p- and s-polarization of the incident light, respectively, and $C_{ELP} = 2\pi d/[\lambda_0 \cos(\Theta_{int})]$. The similarity of eqns. (2) and (3) shows that trends in η or T observed in the two experiments can be directly compared.

The field-dependent steady-state performance was determined by gradually increasing the electric field in steps of 250 V. For each step, the data were taken 5 min after this field had been applied (allowing for the devices to reach quasi-steady-state conditions), and then the next higher field was applied. The temporal evolution of the PR performance was studied by two different methods. In method A, the samples were illuminated uniformly by the '1' write beam without the electric field applied to erase gratings which had been recorded previously and to allow for relaxation of the chromophores to random orientation. With the materials studied here, 10 min were necessary to accomplish that safely. Then, the sample was illuminated with both writing beams for another 15 min, but still without an electric field. Finally, the field was turned on by a reed relay (response time $\ll$1 ms). By measuring the transmission in ELP by the same method, information about the temporal orientation of the chromophores can be obtained. In method B, similarly to method A, pre-existing gratings were erased by illuminating the sample uniformly by the '1' write beam for 10 min without an electric field applied. Then, the devices were poled for 15 min by applying an electric field. During that time, which was long enough to reach the quasi-steady state for poling, the sample was illuminated uniformly by beam '1'. Finally, the second write beam was switched on by a magnetic shutter (opening time *ca.* 2 ms). Method B does not allow one to check the temporal orientation because the samples are prepoled. For both methods, data collection started 10 ms prior to the switching process. The temporal resolution of the set-up was 0.5 μs. For comparison between the different materials we refer to the time necessary to reach 50% of the quasi-steady state value reached at 500 s (τ_{50}).

3 Results and Discussion

3.1 Differential scanning calorimetry

The glass-transition temperatures of the composites were adjusted by adding the appropriate amount of plasticizer. It turned out that with our preparation method the lowest T_g of a DBOP-PPV-based composite which still allowed sufficient dielectric field strength to be applied to the devices was *ca.* 15 °C. The compatibility of the EO chromophore mixture was found to be much better with PVK than with DBOP-PPV, in contrast to our expectations. This is clearly visible in the DSC curves: during cooling, both material classes exhibit only a

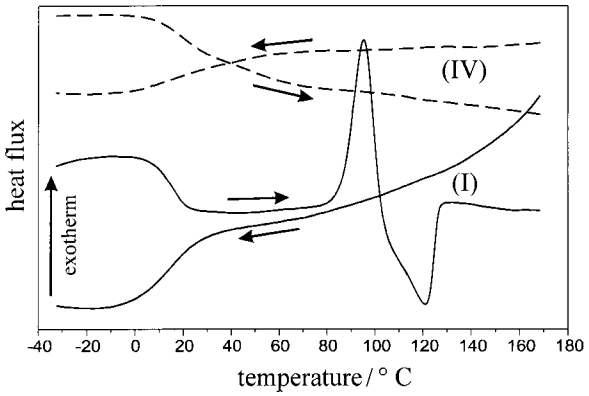

Fig. 2 DSC curves for the DBOP-PPV-based (solid line) and the PVK-based (dashed line) PR composites; heating (cooling) rate 20 (−15) K min^{-1}. The general features (*i.e.*, the occurrence or non-occurrence of the crystallization/melting peaks and T_gs) are identical for all DBOP-PPV- and PVK-based materials.

glass transition. By contrast, upon heating a pair of exothermic/endothermic peaks indicates crystallization and melting, respectively, of the chromophores for the DBOP-PPV-based composite (solid line, Fig. 2), whereas this is barely seen for the PVK-based systems with the temperature schedule used here (dashed line). This incompatibility resulted in a shortened lifetime of the DBOP-PPV- compared with the PVK-based devices at elevated temperature. At room temperature, however, the devices have remained clear for several months so far (DBOP-PPV-based composite) or even for more than 1 year (PVK-based composites).

3.2 Dynamic PR performance

As was pointed out in the Introduction, their slow response is the most prominent weakness of the current organic PR materials. First, we used recording scheme A (field on) to compare the orientational mobilities of the chromophores with the holographic response time. For materials I, II, IV and VI the DFWM response was slower than the temporal change in transmission in ELP (Fig. 3 and 4), indicating that the formation of the space-charge field limited the DFWM response as expected for low-T_g materials. Only on long time scales ($t > 100$ s) did the orientation take over as the limiting process. By contrast, in materials III and V the responses were almost identical in DFWM and ELP, hence these materials were orientation limited. Material VII did not show any PR response.

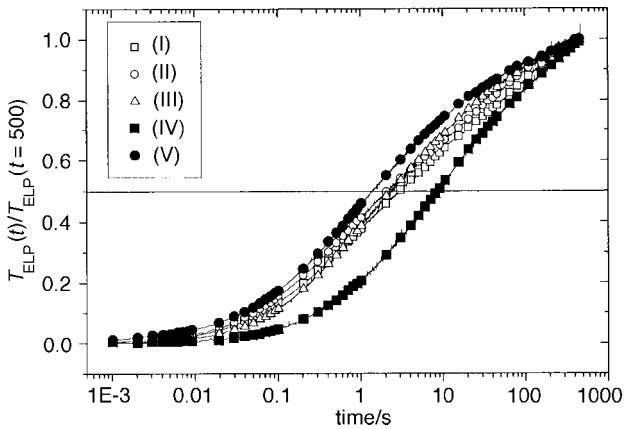

Fig. 3 Dynamic measurement of the transmission in ELP at $E = 62$ V μm^{-1} by method A for the DBOP-PPV based composites (open symbols: I, squares, II, circles, III, triangles) and the PVK-based composites (solid symbols: IV, squares, V, circles). The data are normalized by the quasi-steady-state value obtained at $t = 500$ s.

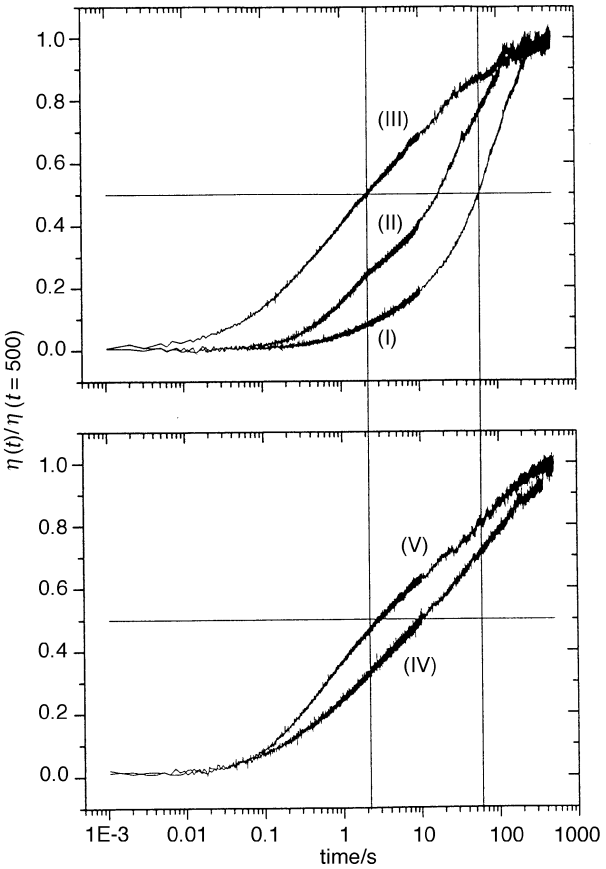

Fig. 4 Dynamic measurement of the diffraction efficiencies η in DFWM obtained by the recording method A at $E = 62$ V μm^{-1} for the DBOP-PPV based materials I–III, top) and the PVK-based composites (IV, V, bottom). The data are normalized by the quasi-steady-state value obtained at $t = 500$ s.

The orientational speed of the chromophores was more than twice as fast in the DBOP-PPV-based materials I–III than in PVK-based material with similar T_g (IV; Table 3). This result can be rationalized by assuming the internal free volume to be larger in the DBOP-PPV-based material, which seems plausible considering the stiff nature of the conjugated chains and the bulky aromatic side groups. Both factors hinder close packing of the polymer chains. Furthermore, owing to the polar nature of the PVK/ECZ-based materials there are dipole–dipole interactions with the chromophores, which also slow orientation. This view is also supported by the fact that the compatibility of the chromophores with PVK/ECZ is better than that with DBOP-PPV owing to the presence of a dipolar interaction with the matrix polymer and the plasticizer. The orientational speed of the softer PVK-based materials V–VII is faster than that in the DBOP-PPV-based composites I–III.

Second, we compared the holographic responses obtained by the two recording schemes. As reported before,[29] method B (second beam on) resulted in a faster recording speed than method A (field on) for all materials (Fig. 4 and 5, Table 3). The enhancement was more than one order of magnitude for the DBOP-PPV-composites I and II, while a factor *ca.* 3 was found for the two PVK-based materials IV and V and for the DBOP-PPV-based material III. The speed enhancement was attributed to the different start conditions prior to the writing process.[29] One reason is that in terms of orientation of the chromophores the start condition is much closer to the steady-state situation in OEM for method B than for method A. As a result, the temporal change in orientation during the grating build-up is faster in method B than in method A, as can be seen, for example, for the orientation-limited materials III and V. The second reason is that unlike in inorganic PR

Table 3 Physical properties of the PR composites I–III

Parameter[a]	Error	(I) DBOP-PPV	(II) DBOP-PPV	(III) DBOP-PPV	(IV) PVK	(V) PVK
T_g/°C	0.2	14.3	15.3	14.4	15.1	10.9
α_t at 633 nm/cm^{-1}	1	8	15	34	16	15
α_s at 633 nm/cm^{-1}	1	3[b]	10[b]	29[b]	11	10
$E(\eta_{max})$/V μm^{-1}	2	63	64	62	71	68
$E(T_{max})$/V μm^{-1}	2	64	67	64	82	75
$E(T_{max})/E(\eta_{max})$		1.02	1.08	1.08	1.15	1.10
Δn	0.07	2.44	2.44	2.60	1.98	2.16
ϕ	5%	22	20	11	24	22
E_q/V μm^{-1}	10%	153	170	320	140	153
E^*/V μm^{-1}		57.5	58.3	60.9	56.6	57.5
τ_{50}(ELP)/s (method A)	0.5	3.0	2.2	2.5	9.0	1.4
τ_{50}(DFWM)/s (method A)	0.2	59	18	2.3	10.0	3.0
τ_{50}(DFWM)/s (method B)	0.2	3.6	1.7	0.6	3.3	1.0

[a] Glass-transition temperature, T_g, total absorption coefficient, α_t, sensitizer absorption coefficient, α_s, field for maximum diffraction efficiency in DFWM experiments, $E(\eta_{max})$, field for maximum transmission in ELP experiments, $E(T_{max})$, and ratio $E(T_{max})/E(\eta_{max})$. The following refer to an electric field of $E = 62$ V μm^{-1}: refractive index index modulation Δn, phase shift ϕ, saturation field E_q, field E^* according to eqn. (4), orientational response time τ_{50} in ELP experiments (corresponds to method A), holographic response time τ_{50} in DFWM experiments using recording method A, holographic response time τ_{50} in DFWM experiments using recording method B. [b] Absorption of PCBM + absorption of the DBOP-PPV (50% m/m yield 3 cm^{-1}).

crystals, charge-carrier generation is relatively poor.[1–6,30] The carriers have to be generated before the PR space-charge field can fully develop. In particular, relatively few charge carriers are initially present in method A, since the field is zero before recording starts. By contrast, a much larger number of carriers has already been generated when the second beam is switched on in method B, because the field was applied and the sample was illuminated uniformly. This is proved by the fact that the speed enhancement obtained when using method B rather than A is higher for the materials I and II, which have the poorest charge-generation efficiency (see below).

For comparison of PR performance of the DBOP-PPV-based and the PVK-based composites, we first consider the two materials without sensitizer. Whereas the DBOP-PPV-based material I showed a reasonable PR performance (Fig. 3–6), the corresponding PVK-based material VII did not show any notable PR effect while having a similar ELP performance. Since the PVK-based material without TNF shows no PR effect, we can exclude that the chromophores DMNPAA and MNPAA (Fig. 1) act as sensitizers. Therefore, the reason for the different behaviors of the materials must be

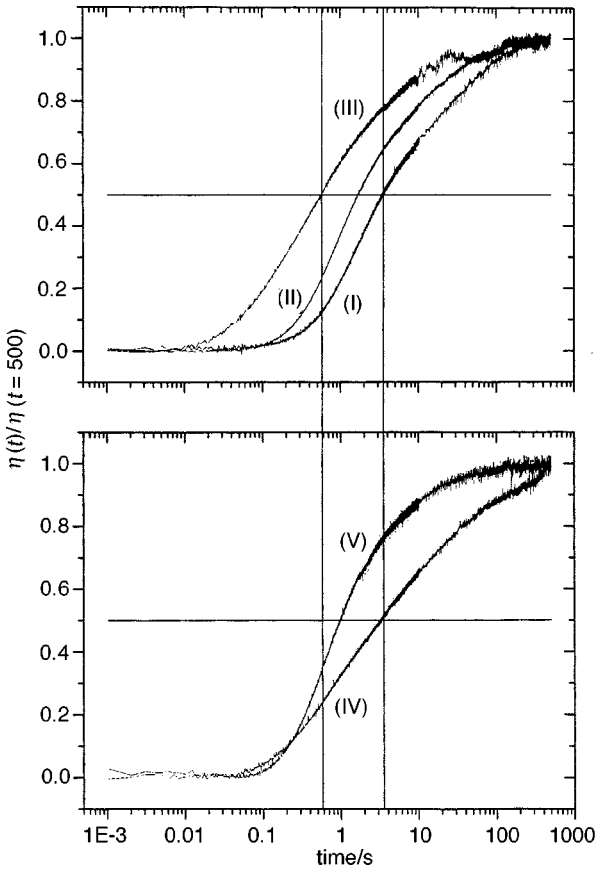

Fig. 5 Dynamic measurement of the diffraction efficiencies η in DFWM obtained by the recording method B at $E = 62$ V μm^{-1} for the DBOP-PPV based materials (I–III, top) and the two PVK-based composites (IV, V, bottom). The data are normalized by the quasi-steady-state value obtained at $t = 500$ s.

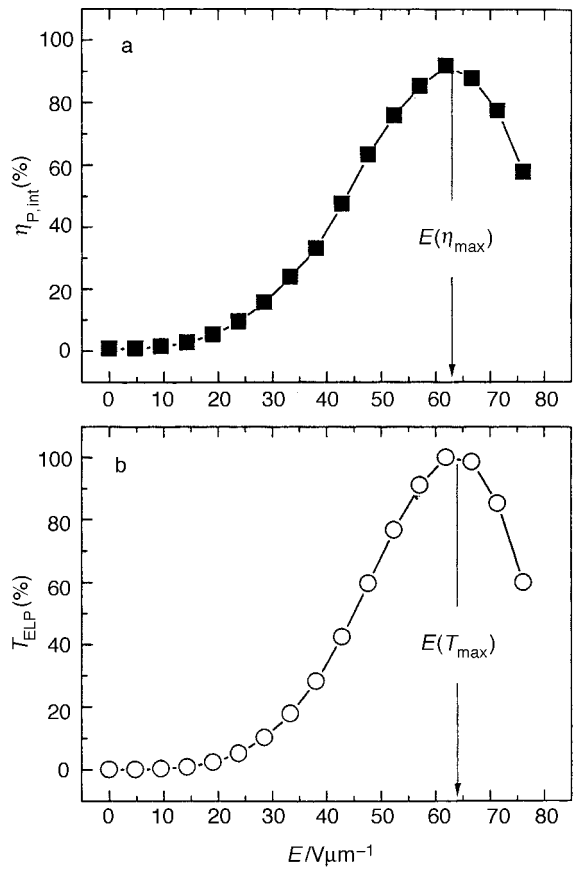

Fig. 6 Steady-state performance for the DBOP-PPV-based PR composite I as a function of the applied electric field E: (a) internal diffraction efficiency $\eta_{P,int}$ in DFWM experiments (solid squares) and (b) transmission T in ELP experiments (open circles).

the difference in the absorption coefficients of the two polymers at the laser wavelength used, 633 nm. In contrast to PVK with $\alpha(633\ \text{nm}) \approx 0$, DBOP-PPV has an absorption coefficient of 6 cm^{-1} and can thus be directly photoexcited.

Second, we compared the composites II and IV with similar T_gs and absorption coefficients. As mentioned above, even though the T_gs are similar, the PVK based material shows a slower orientational speed and has an orientation-limited dynamic performance. Hence, the influence of the electronic properties (charge generation and redistribution) on the dynamic performance of this material cannot be compared, since only the DBOP-PPV-based material is limited by these factors.

The next step was to compare the material II with the further plasticized PVK based material V. Again, both materials have similar absorption coefficients, but material V has a 4 °C lower T_g. The DFWM response using method B of the DBOP-PPV-based composite II is about a factor of 2 slower than for the PVK-based system V. Since the response of these two materials is limited by the build-up of the space-charge field, either charge generation or charge transport should be responsible for this. Xerographic discharge measurements revealed a generation efficiency Φ of about 10^{-2} in PVK/TNF-based PR composites at $E = 100$ V μm^{-1}, whereas $\Phi < 10^{-4}$ was estimated in DBOP-PPV/C_{60} under similar conditions.[31] One reason for this finding is the higher molecular mass of [6,6]PCBM (910 g mol^{-1}) compared with TNF (314 g mol^{-1}), resulting in a three times higher number density of TNF/carbazole complexes for equal mass content such as in materials II and V. Furthermore, the difference between the oxidation potential of the hole conducting polymer (acting as the donor, see Table 1) and the reduction potential of the sensitizer (acting as the acceptor; $E^{\circ}_{red} = -0.49$ V for TNF and -0.82 V for [6,6]PCBM[26] both *vs.* Ag/AgCl as the reference electrode) is larger for DBOP-PPV/[6,6]PCBM ($\approx$1.8 eV) than for PVK/TNF ($\approx$1.6 eV). Therefore, the electron transfer is expected to be less efficient in DBOP-PPV/PCBM. However, both arguments seem insufficient to explain fully the large discrepancy in charge-carrier generation efficiency observed for the materials. The exact reason is currently unknown, but it can most probably be attributed to the fact that PVK and TNF form a charge-transfer (CT) complex, which is a very favorable situation owing to partial electron transfer in the ground state. We tried to improve Φ in the DBOP-PPV-based system by using a number of sensitizers such as various pigment dyes typically used for xerographic applications, and also the "normal" unsubstituted fullerene C_{60}, but without success. C_{60} showed poor compatibility with DBOP-PPV, resulting in highly scattering materials even for concentrations as low as 0.05% m/m. In the other cases, the sensitivity was lower than with [6,6]PCBM. We checked also the use of [6,6]PCBM as a sensitizer in a PVK-based composite (material VI). The holographic response was found to be more than two orders of magnitude slower than in the corresponding material with identical T_g and sensitized with TNF (material V), whereas the ELP performance was very similar. Hence, this finding can be unambiguously attributed to the poor sensitization of the PVK by [6,6]PCBM.

Finally, we compared the soft PVK-based material V with the DBOP-based material III, which have a similar number density of sensitizer moieties, assuming that most of the TNF molecules form a CT complex with carbazole units which is a good approximation for low TNF content. The DFWM response of the highly absorbing material III is slightly faster than that for the PVK-based system V. However, as mentioned above, since material III is orientation limited, the influence of the build-up time of the space-charge field on the dynamic performance of this material cannot be compared with V, since only the latter material is limited by these factors. As mentioned above, the T_g of the DBOP-based composites could not be lowered further without risking dielectric breakdown.

As a preliminary conclusion of this section, the reduced charge-carrier generation efficiency in the DBOP-PPV-based systems I and II explains two experimental findings: (i) that the enhancement of the holographic recording speed going from method A to method B is much stronger for the DBOP-PPV-based materials I and II than for the soft PVK-based system V and the better sensitized DBOP-PPV-based material III and (ii) the much faster response of the TNF-sensitized PVK-based systems compared with the DBOP-PPV-based materials I and II using method A. The fact, that the response times using method B are of the same order of magnitude for all materials indicates that the hole mobilities are similar in the DBOP-PPV- and the PVK-based composites. This is despite the fact that the photoconductivity (determined by measuring over a gap of 200 μm) is more than one order of magnitude larger in DBOP-PPV than in PVK.[24] We attribute this discrepancy to a difference in the T_g dependence of μ_h in PVK and DBOP-PPV.

3.3 Steady-state PR performance

Fig. 6(a) shows a typical curve of the steady-state diffraction efficiency η as a function of the applied electric field (squares) for material **I**. It increases with increasing external field for all composites under investigation and finally reaches a maximum for a specific field value $E(\eta_{max})$ in accordance with eqn. (2). $E(\eta_{max})$ is lowest for the composites based on DBOP-PPV (Table 3). Since the experimental geometry and device thickness are identical, the index modulation Δn achieved at $E(\eta_{max})$ is also similar [$\Delta n(\eta_{max}) \approx 2.6 \times 10^{-3}$]. Hence, the lower $E(\eta_{max})$ for DBOP-PPV-based composites I–III indicates better PR performance than for the PVK-based composites IV and V. A possible origin of this finding is differences in the quality of orientation of the chromophores in the two matrices. A first indication for this interpretation was already mentioned above, *i.e.*, the faster orientational speed of the chromophores in the DBOP-PPV-based materials I–III compared with the PVK-based system with identical T_g (IV). However, this argument cannot explain the remaining difference between the materials I–III and V since the orientation is faster in V (Table 3, Fig. 3). Therefore, we checked the degree of orientation by ELP experiments by determining the fields of maximum transmission $E(T_{max})$. Similarly to $E(\eta_{max})$ in DFWM experiments, a lower $E(T_{max})$ in ELP indicates higher non-linearity (for an identical chromophore content as in our case). We obtained $E(T_{max} = 65, 69$ and $69)$ V μm^{-1} for the DBOP-PPV-based composites I, II and III, respectively, and $E(T_{max}) = 82$ and 75 V μm^{-1} for the PVK-materials IV and V, respectively. In other words, for a given field, the poling-induced index change $\Delta n'$ is larger in the DBOP-PPV-based composites, even larger than in the softer PVK-based composite V. The ratio $E(T_{max})/E(\eta_{max})$ can help to compare the relative degree of orientation. It is very similar for all materials ($\approx$1.1; see Table 3). This indicates that differences in the degree of orientation can at least partly explain the observed differences in the steady-state PR performance of the materials.

The latter could also result from different bulk refractive indices of the composites. In the tilted geometry used here for DFWM and ELP, a lower refractive index would yield a more favorable internal tilt angle of the gratings for constant external geometry owing to Snell's law. However, the indices of the pristine polymers are very close: $n \approx 1.68$ was found at 633 nm for poly[1,4-phenylene-1,2-di(4-phenyloxy)vinylene] (DPOP-PPV),[32] which differs from DBOP-PPV by two methylene groups, and n(PVK) ≈ 1.65 according to the sup-

plier (Aldrich). Assuming similar changes of the refractive index of the two materials in the presence of the chromophores (which leads to an increase in n due to their dipolar character[33]), plasticizer and sensitizer, the difference in refractive indices between the two material classes should remain close to 0.003 as for the pristine polymers. Hence, the influence of the bulk refractive index is expected to be negligible.

Finally, differences in the amplitude of the PR space-charge field E_{SC} might be the reason for the difference in PR performance. At $E(\eta_{max})$, charge-carrier migration is the transport process dominating the formation of E_{SC}, and diffusion can be neglected to a good approximation. Under these conditions and in the small modulation limit, the amplitude of E_{SC} takes the form[34]

$$|E_{SC}| \approx C \overbrace{\frac{2\sqrt{I_1 I_2}}{I_1 + I_2}}^{m} \overbrace{\frac{\sigma_{ph}}{\sigma_{ph} + \sigma_d}}^{M} \overbrace{\left[\frac{E_0^2}{1(E_0/E_q)^2}\right]^{1/2}}^{E^*} \quad (4)$$

where m ($\leqslant 1$) is the contrast factor of the interference pattern for s-polarized beams, $M(\leqslant 1)$ is the "conductivity contrast", σ_d and σ_{ph} are the dark and the photoconductivity, respectively, $E_0 = E_{ext}\cos(\varphi)$ is the projection of the external electric field E_{ext} on to the grating wave vector, $\varphi = (\pi - \alpha_1 - \alpha_2)/2$ is the grating tilt angle and $E_q = eN_T/K\varepsilon_r$ is the saturation field, e being the elementary charge, N_T the number density of traps, ε_r the bulk permittivity (dielectric constant) and K the grating wavenumber. $C = 1$ (0.5) for linear (quadratic) recombination of the charge carriers.

The contrast factor was constant ($m \approx 1$) in all cases. For the PVK-based materials IV and V we found $C \approx 1$ and $M \approx 1$. Similar results are expected for the DBOP-PPV-based composites I–III. Therefore, we concentrate on the field term E^* in eqn. (4). One important factor is the matrix polarity ε_r. To probe it we incorporated a small amount of the highly solvatochromic dye 5-dimethylamino-5′-nitro-2,2′-bithiophene,[35] in the two matrix polymers. λ_{max} was determined as 542 (537) nm in PVK (DBOP-PPV). Longer t_{max} corresponds to higher polarity. In the presence of the respective plasticizer we obtained 542 (538) nm for PVK/ECZ (DBOP-PPV/DPP). Thus, as expected the polarity of the DBOP-PPV-based composites is slightly increased in the presence of DPP, while the presence of ECZ used as a plasticizer in the PVK-based composites leaves the polarity unchanged. The absolute values of λ_{max} indicate that the polarity of both composite classes is somewhere between those of dichloroethane (537 nm) and *N*,*N*-dimethylformamide (DMF) (549 nm) and slightly (but significantly) lower in the DBOP-PPV-based composites (assuming again similar changes by the chromophores; see above). This finding suggests that the effective field inside the DBOP-PPV-based composite is slightly stronger than in PVK-based materials for the same external field in agreement with our observation of a better steady-state PR performance for the DBOP-PPV system. Nevertheless, the overall influence of polarity on the PR performance of the two material classes probably remains small.

The second factor that might influence E^* is the trap density, which determines the saturation field E_q. This in turn should affect the phase shift ϕ between the light intensity pattern and the recorded index modulation. ϕ is given by

$$\phi = \text{atan}(E_0/E_q) \quad (5)$$

when E_D is neglected.[9,34] This is a good approximation under our experimental conditions, *i.e.*, with relatively high electric fields applied ($E_0, E_q \gg E_D$). ϕ was determined by the moving grating technique[36] and the results are given in Table 3. The phase shift is smaller in the DBOP-PPV-based than in the PVK-based materials, indicating a stronger E_q in the DBOP-PPV-system, as follows from eqn. (5). Using eqn. (4), we calculated E^* at $E_0 = 62$ V μm^{-1} for the PVK-based (DBOP-PPV-based) materials (see Table 3). It is obvious that E^* is slightly stronger in the DBOP-PPV-based materials, which is again in agreement with our experimental observation. Furthermore, E^* increases with increasing sensitizer (PCBM) content in the DBOP-PPV-based composites.

We conclude that the number density of traps N_T is generally larger in DBOP-PPV-based than in PVK-based composites. Recently, we have found experimental evidence that the traps in amorphous organic PR materials are conformational traps,[37] *i.e.*, charges are trapped on transport moieties which have poor electronic overlap with the neighboring hopping sites. In conjugated polymers hole mobility along the effectively conjugated polymer segments is expected to be relatively high, but hopping between the conjugated segments and chains still remains the process that limits charge transport. Since the π-conjugated chains are long and stiff, situations with poor electronic overlap are likely, in particular considering the bulky side groups in DBOP-PPV. Therefore, it seems plausible that conformational traps occur more frequently than in a material containing small transport moieties such as PVK, in particular considering the fact that the latter composites contain additional independent charge-transport moieties (ECZ).

4 Conclusion

We have compared the performance of low-T_g (10–15 °C) PR polymer composites based on different photoconductors. One contained isolated charge-transport moieties for hopping (the commonly used PVK) and the other was based on a π-conjugated polymer (the PPV derivative DBOP-PPV). It became obvious that the general hopes of using π-conjugated polymers for PR applications were too high in the case studied here. Regarding the steady-state PR performance, the DBOP-PPV-based composites were found to be superior to the two PVK-based systems with identical or even lower T_g. Three factors turned out to be responsible for this result: (i) the slightly reduced polarity of the DBOP-PPV/DPP matrix, (ii) the larger trap density, and (iii) the improved degree of orientation that can be achieved in DBOP-PPV/DPP-based compared with the PVK/ECZ-based systems. We attribute the last factor to the larger internal free volume and reduced dipolar chromophore–matrix interaction in the DBOP-PPV/DPP matrix as discussed above.

In terms of DFWM response time, the performance of the DBOP-PPV-based composite was found to be similar to that of PVK-based materials despite the higher hole-drift mobility reported for the pristine polymer. It should be emphasized that the detailed considerations discussed above strictly apply only to the wavelength used here (633 nm) and have to be re-evaluated for every other wavelength. One of the major tasks for the future will therefore be to find better donor–acceptor combinations to improve sensitization.

5 Acknowledgements

This work was supported by the "Photonic" program of the Volkswagen Foundation (Germany). We thank Dr. D. Neher (Max-Planck Institute for Polymer Research, Mainz, Germany) and R. Bittner (University of Munich) for very fruitful discussions, Dr. F. Würthner (Organic Chemistry Department, University of Ulm, Germany) for providing 5-dimethylamino-5′-nitro-2,2′-bithiophene and Dr. C. Brabec (Physical Chemistry Department, University of Linz, Austria) for logistic help. J. C. H. thanks NOVEM (The Netherlands Agency for Energy and the Environment) for financial support (grant No. 146.120-008.1).

References

1 W. E. Moerner and S. M. Silence, *Chem. Rev.*, 1994, **94**, 127.
2 Y. Zhang, R. Burzynski, S. Ghosal and M. K. Casstevens, *Adv. Mat.*, 1996, **8**, 111.
3 B. Kippelen, K. Meerholz and N. Peyghambarian, in *Nonlinear Optics of Organic Molecules and Polymers*, ed. H. S. Nalva and S. Miyata, CRC Press, Boca Raton, FL, 1997, ch. 8.
4 K. Meerholz, *Angew. Chem.*, 1997, **109**, 981; *Angew. Chem., Int. Ed. Engl.*, 1997, **109**, 945.
5 W. E. Morner, A. Grunnet-Jepsen and C. L. Thompson, *Annu. Rev. Mater. Sci.*, 1997, **27**, 585.
6 K. Meerholz, B. Kippelen and N. Peyghambarian, in *Photonic Polymer Systems*, ed. D. L. Wise, G. E. Wnek, D. J. Trantolo, T. M. Cooper and J. D. Gresser, Marcel Dekker, New York, 1998, ch. 15.
7 K. Meerholz, B. Volodin, Sandalphon, B. Kippelen and N. Peyghambarian, *Nature* (*London*), 1994, **371**, 497.
8 (a) R. Wortmann, C. Poga, R. J. Twieg, C. Geletneky, C. R. Moylan, P. M. Lundquist, R. G. DeVoe, P. M. Cotts, H. Horn, J. E. Rice and D. M. Burland, *J. Chem. Phys.*, 1996, **105**, 10623; (b) P. M. Lundquist, R. Wortmann, C. Geletneky, R. J. Twieg, M. Jurich, V. Y. Lee, C. R. Moylan and D. M. Burland, *Science*, 1996, **247**, 1182.
9 A. Grunnet-Jepsen, C. L. Thompson, R. J. Twieg and W. E. Moerner, *Appl. Phys. Lett.*, 1997, **70**, 1515.
10 F. Würthner, R. Wortmann, R. Matschiner, K. Lukaszuk, K. Meerholz, Y. De Nardin, R. Bittner, C. Bräuchle and R. Sens, *Angew. Chem. Int. Ed. Engl.*, 1997, **36**, 2765; (b) K. Meerholz, Y. De Nardin, R. Bittner, F. Würthner and R. Wortmann, *Appl. Phys. Lett.*, 1998, **73**, 4.
11 B. Kippelen, S. R. Marder, E. Hendrickx, J. L. Maldano, G. Guillernet, B. L. Volodin, D. Steele, Y. Enami, Sandalphon, Y. J. Yao, J. F. Wang, H. Röckel, L. Erskine and N. Peyghambarian, *Science*, 1998, **279**, 54.
12 D. Wright, M. A. Diaz-Garcia, J. D. Casperson, M. DeClue and W. E. Moerner, *Appl Phys. Lett.*, 1998, **73**, 1490.
13 W. E. Moerner, S. M. Silence, F. Hache and G. C. Bjorklund, *J. Opt. Soc. Am. B*, 1994, **22**, 320.
14 H. J. Bolink, V. V. Krasnikov, G. G. Malliaras and G. Hadziioannou, *J. Phys. Chem.*, 1996, **100**, 16356.
15 R. Bittner, C. Bräuchle and K. Meerholz, *Appl. Opt.*, 1998, **37**, 2843.
16 B. Swedek, N. Cheng, Y. Cui, J. Zieba, J. Winiarz and P. N. Prasad, *J. Appl. Phys.*, 1997, **82**, 5923.
17 (a) P. M. Borsenberger and D. S. Weiss, *Organic Photoreceptors for Imaging Systems*, Marcel Dekker, New York, 1993; (b) H. Bässler, *Phys. Status. Solidi. B*, 1993, **175**, 15.
18 (a) O. Zobel, M. Eckl, P. Strohriegel and D. Haarer, *Adv. Mater.*, 1995, **7**, 911; (b) C. Poga, P. M. Lundquist, V. Lee, R. M. Shelby, R. J. Twieg and W. E. Moerner, *App. Phys. Lett.*, 1996, **69**, 1047; (c) S. Schloter and D. Haarer, *Adv. Mater.*, 1997, **9**, 991.
19 (a) S. Ducharme, J. C. Scott, R. J. Twieg and W. E. Moerner, *Phys. Rev. Lett.*, 1991, **66**, 1846; (b) S. M. Silence, C. A. Walsh, J. C. Scott, T. J. Matray, R. J. Twieg, G. C. Bjorklund, F. Hache and W. E. Moerner, *Opt. Lett.*, 1992, **17**, 1107.
20 (a) Y. Cui, Y. Zhang, P. N. Prasad, J. S. Schildkraut and D. J. Williams, *Appl. Phys. Lett.*, 1992, **61**, 2132; (b) K. Ogino, T. Nomura, T. Shichi, S.-H. Park, H. Sato, T. Aoyama and T. Wada, *Chem. Mat.*, 1997, **9**, 2768.
21 (a) Y. Zhang, S. Ghosal, M. K. Casstevens and R. Burzynski, *Appl. Phys. Lett.*, 1995, **66**, 256; (b) S. M. Silence, J. C. Scott, J. J. Stankus, W. E. Moerner, C. R. Moylan, G. C. Bjorklund and R. J. Twieg, *J. Phys. Chem.*, 1995, **99**, 4096; (c) L. Wang, Y. Zhang, T. Wada and H. Sasabe, *Appl. Phys. Lett.*, 1996, **69**, 728; (d) L. Wang, Y. Zhang, T. Wada and H. Sasabe, *Appl. Phys. Lett.*, 1997, **70**, 2949; (e) H. Bolink, C. Arts, V. Krasnikov, G. Malliaras and G. Hadziioannou, *Chem. Mater.*, 1997, **9**, 1407.
22 (a) Z. Peng, A. R. Gharavi and L. Yu, *Appl. Phys. Lett.*, **69**, 4002 (1996); (b) Z. Peng, A. R. Gharavi and L. Yu, *J. Am. Chem. Soc.*, 1997, **119**, 4622.
23 (a) H. H. Hörhold and M. Helbig, *Makromol. Chem. Macromol. Symp.*, **12**, 229 (1987); (b) H. H. Hörhold, A. Bleyer, E. Birckner, S. Heinze and F. Leonhardt, *Synth. Met.*, 1995, **69**, 525; (c) F. Leonhardt, PhD Dissertation, University of Jena, 1990.
24 H. H. Hörhold, unpublished results.
25 K. Meerholz, Y. De Nardin and R. Bittner, *Mol. Cryst. Liq. Cryst.*, 1998, **315**, 99.
26 J. C. Hummelen, B. W. Knight, F. LePeq and F. Wudl, *J. Org. Chem.*, 1995, **60**, 532.
27 H. Kogelnik, *Bell Syst. Tech. J.*, 1969, 2909.
28 (a) C. C. Teng and H. T. Man, *Appl. Phys. Lett.*, 1990, **56**, 1734; (b) J. S. Schildkraut, *Appl. Opt.*, 1990, **29**, 2839.
29 E. Mecher, R. Bittner, C. Bräuchle and K. Meerholz, *Synth. Met.*, in the press.
30 A. Mozumder, *J. Chem. Phys.*, 1974, **60**, 4300.
31 T. Däubler, D. Neher, R. Bittner and K. Meerholz, unpublished results.
32 T. Gabler, R. Waldhäusl, A. Bräuer, F. Michelotti, H. H. Hörhold and U. Bartuch, *Appl. Phys. Lett.*, 1997, **70**, 928.
33 B. Kippelen, Sandalphon, B. Volodin, K. Meerholz and N. Peyghambarian, *ACS Symp. Ser.*, 1996, **672**, 218.
34 N. V. Kukhtarev, V. B. Markov, S. G. Odulov, M. S. Soskin and V. L. Vinetskii, *Ferroelectrics*, 1979, **22**, 949.
35 (a) F. Effenberger and F. Würthner, *Angew. Chem.*, 1993, **105**, 742; (b) F. Effenberger, F. Würthner and F. Steybe, *J. Org. Chem.*, 1995, **60**, 2082.
36 (a) K. Sutter, J. Hulliger and P. Günter, *Solid State Commun.*, 1990, **7**, 867; (b) C. A. Walsh and W. E. Moerner, *J. Opt. Soc. Am. B*, 1992, **90,** 1642.
37 R. Bittner, T. Däubler, D. Neher and K. Meerholz, *Adv. Mater.*, 1999, **11**, 123.

Paper 8/09732A